Interner Bericht
F 32-2
Juli 1967

PHOTOPRODUCTION OF ρ^0 MESONS ON HYDROGEN, CARBON AND ALUMINIUM WITH PHOTONS OF KNOWN ENERGY AND EVIDENCE OF K^0 AND Φ PHOTOPRODUCTION

by

H. Blechschmidt, J.P. Dowd[+], B. Elsner, K. Heinloth, K.H. Höhne, S. Raither, J. Rathje, D. Schmidt, J.H. Smith[++], J.H. Weber

Deutsches Elektronen-Synchrotron DESY, Hamburg, Germany

[+] Present address: SMTI, New Bedford, Massachusetts, U.S.A.

[++] Present address: University of Illinois, Urbana, Illinois, U.S.A.

In a spark chamber experiment photoproduction of pion pairs on hydrogen, carbon and aluminium has been investigated at photon energies between 3.2 and 4.4 GeV. For each event the photon energy was measured with an accuracy of ±50 MeV.

(1) $$\gamma + A \rightarrow A + \pi^+ + \pi^-$$

Mainly the production of ρ^o mesons

(2) $$\gamma + A \rightarrow A + \rho^o$$

has been studied. In addition we observed the production of K^o mesons and Φ mesons.

1. Experimental Setup

The experimental setup is shown in Fig. 1. A bremsstrahlung beam of $2 \cdot 10^5$ effective quanta/sec is produced by conversion of a 4.4 GeV positron beam in the tantalum target TA. The energy of the photon is determined by measuring the momenta of the associated positrons[1]. This is done using a horizontally focusing bending magnet MD and an array of 29 scintillation counters (tagging system).

The positron beam intensity is monitored by the ionization chamber I.CH. which was calibrated against a quantameter during the

experiment. The photon beam is absorbed inside the magnet MH by the tungsten block A.

In the detection apparatus[2] consisting of two pairs of spark chambers and the deflection magnet MH production angles and momenta of the produced charged particles are measured. Pions are identified by a threshold Čerenkov counter Č and two thick plate spark chambers SC5 and SC6. Pictures were taken whenever two charged particles passed the spark chamber system. Out of the 13,000 pictures taken we got 1,500 events for our analysis.

The acceptance Acc of our apparatus for detecting a two particle system was calculated as a threefold integral over:

1) azimuthal angle and polar angle θ_N^* of the positive particle in the two particle rest system with respect to the direction of the recoiling target particle and

2) the azimuthal angle of the combined system.

In the case of ρ^o and Φ meson production a $\sin^2$ distribution was assumed for the polar angle θ_N^* due to previous measurements on the ρ^o [3]. In the case of K^o production we assume isotropy.

In the calculation of the acceptance Acc' for detecting the decay particles as a function of their polar angle the integration over θ_N^* is omitted.

2. Results

2.1. ρ Meson Production

To separate the process (1) from reactions where additional particles were produced we consider the difference Δk between the measured photon energy and the photon energy computed from the measured momenta of the two pions under the assumption that the process (1) has occurred. From the Δk distribution shown in Fig. 2 we deduce that all the events which are in the range from $-0.2\ \text{GeV} < \Delta k < +0.2\ \text{GeV}$ are due to the reaction (1).

The invariant mass spectrum of the two pion system produced on H_2, C and Al is shown in Fig. 3. The mass and width[3] of the ρ^o meson results in:

$$m_\rho = 734 \pm 12\ \text{MeV} \quad \text{for } H_2$$

$$m_\rho = 755 \pm 12\ \text{MeV} \quad \text{for C}$$

$$m_\rho = 758 \pm 12\ \text{MeV} \quad \text{for Al}$$

These values are in agreement with earlier photoproduction results[4,5,6,7,8]. An averaged value for the width of the ρ^o meson is $\Gamma = 0.15 \pm 0.03$ GeV. On the basis of the photon dissociation model, Ross and Stodolsky[9] predict that the mass distribution for photoproduced ρ^o mesons shows a Breit-Wigner behaviour multiplied with an additional factor $\frac{1}{m_{\pi\pi}^4}$. Using this correlation

we get a shift of the ρ mass to higher values by about 20 MeV and the implication that more than 95 % of our events are due to ρ^o meson production.

The differential cross section $\frac{d\sigma}{dt}$ as a function of the square of the four momentum transfer t to the recoil nucleon is shown for the different targets in Fig. 4. Since our data show the typical diffraction behaviour[10,11] we fitted them with:

$$\frac{d\sigma}{dt} = a \cdot e^{bt} \quad \frac{\text{mb}}{\text{GeV}^2 \text{ nucleus}}$$

This gives the following values:

$a = 0.119 \pm 0.01 \frac{\text{mb}}{\text{GeV}^2}$ $\quad b = 8.1 \pm 1.5 \text{ GeV}^{-2}$ for H_2

$a = 7.4 \pm 0.7 \frac{\text{mb}}{\text{GeV}^2 \text{ nucleus}}$ $\quad b = 47.8 \pm 4.6 \text{ GeV}^{-2}$ for C

$a = 28.0 \pm 3 \frac{\text{mb}}{\text{GeV}^2 \text{ nucleus}}$ $\quad b = 73.0 \pm 9.3 \text{ GeV}^{-2}$ for Al

We find the coefficient b proportional to $A^{\frac{2}{3}}$ where A is the mass number of the target nuclei. a is found to be proportional to $A^{1.65 \pm 0.1}$. This shows a behaviour of the nucleus between opacity and transparency.

The total cross section for the process $\gamma + A \rightarrow \rho^o + A$ was determined by extrapolation of the differential cross section $\frac{d\sigma}{dt}$

to high $|t|$ values and integration over t. In the energy region $3.2 < E\gamma < 4.4$ GeV we get the values:

$$\sigma_{tot} = 13.9 \pm 1.8\ \mu b \qquad \text{for } H_2$$

$$\sigma_{tot} = 117 \pm 22\ \frac{\mu b}{\text{nucleus}} \qquad \text{for C}$$

$$\sigma_{tot} = 250 \pm 40\ \frac{\mu b}{\text{nucleus}} \qquad \text{for Al}$$

The angular distribution $\frac{d\sigma}{d\Omega^*}$ of the ρ^o mesons in the center of mass system for the different targets is shown in Fig. 5. The values for hydrogen are in good agreement with bubble chamber results[4].

Figs. 6a and 6b show the angular distribution of the decay pions in the ρ^o rest system. θ_N^* is the angle between the positive pion and the outgoing target particle whereas θ_γ^* is the angle of the positive pion with respect to the direction of the incoming photon.

Our apparatus accepts a range for both the polar angles θ_γ^* and θ_N^* of about $-.4 < \cos\theta < +.4$ for the carbon and aluminium target and of $-.6 < \cos\theta < +.6$ for the hydrogen target.

Bubble chamber results[4] show a $\sin^2$ dependence for θ_N^* and isotropy for θ_γ^*. Within our limitted range of acceptance our results are compatible with these data.

In all figures and calculations we have neglected those few events the acceptance of which was less than 1 % of the mean value.

2.2. K^o Production

Besides the ρ^o production we expect also some information on photoprocution of K^o mesons. These K^o mesons could be detected via the decay into two charged pions:

$$(3) \qquad \gamma + p \rightarrow K^o + X, \qquad K^o \rightarrow \pi^+ + \pi^-$$

To separate the K^o production from the much more copious ρ^o production we looked for pion pairs originating between the hydrogen target and the first spark chamber. Here the background arises mainly from ρ^o production on air which is much smaller than on the hydrogen target. From the lifetime of the short living K^o we calculated that 48 % of all K^o mesons produced in the target decay in this region. Because the K^o meson has to be produced

together with a strange particle we only show in Fig. 7 the mass distribution of two pion events for those events in which the recoil mass is higher than 1.1 GeV. There is an enhancement in the distribution between 0.45 and 0.5 GeV which we claim to be mainly due to K^o production. For these events the mass distribution of the recoil system is shown in Fig. 8.

We see that the photoproduction of K^o mesons is more likely to go with a heavy recoil system ($m_X > 1.35$ GeV) than with a Σ^+. The resulting differential cross section averaged over CMS angles from 0^o - 14^o for photon energies between 3.2 and 4.4 GeV is:

$$\left(\frac{d\sigma}{d\Omega^*}\right)_{0^o-14^o} = 0.2 \pm 0.2 \text{ μbarn/sterad for } \gamma + p \to K^o + \Sigma^+$$

$$\left(\frac{d\sigma}{d\Omega^*}\right)_{0^o-14^o} = 3.2 \pm 2 \text{ μbarn/sterad for } \gamma + p \to K^o + X$$

$$\text{with } m_X > 1.35 \text{ GeV}$$

2.3. Φ Meson Production

To investigate Φ production we looked for K meson pairs in a sample of events in which none of both particles were identified as pions or electrons. Since the expected ratio of K mesons to pions is very small we still have to deal with pion contamination. To resolve the reaction

(4)
$$\gamma + A \to A + \Phi \quad \Phi \to K^+ + K^-$$

from the background we calculate the difference Δk of the known photon energy and the photon energy computed from the measured momenta under the assumption that process (4) has occurred. From kinematical considerations it follows that the pion contamination arises mainly in the region of negative Δk. Therefore we restrict our investigation to events for which Δk is positive. The resulting (K^+K^-) mass distribution is shown in Fig. 9. The peak in the region of 1.02 GeV contains the possible candidates for Φ mesons. To resolve process (4) where the recoil particle is the bare nucleus the distribution of Δk for the remaining 13 events is plotted in Fig. 10. The calculated resolution and the comparison with the resolution of ρ^o meson production (see Fig. 2) allows us to identify events with $\Delta k < .2$ GeV as belonging to reaction (4). The remaining 10 events cover a range of the square of the four momentum transfer to the target particle of $0.02 \lesssim |t| \lesssim 0.035$ GeV^2 which is given by the acceptance. If we divide our events corresponding to the three targets and correct for the undetected events with negative Δk we get the following differential cross sections:

$$\frac{d\sigma}{dt} = (4 \pm 3)\ \frac{\mu b}{GeV^2} \qquad \text{for } H_2 \qquad 0.025 \lesssim |t| \lesssim 0.035\ \{GeV^2\}$$

$$\left.\begin{aligned} \frac{1}{A}\frac{d\sigma}{dt} &= (4 \pm 3)\ \frac{\mu b}{GeV^2\ \text{nucleon}} \quad \text{for C} \\ \frac{1}{A}\frac{d\sigma}{dt} &= (7 \pm 4)\ \frac{\mu b}{GeV^2\ \text{nucleon}} \quad \text{for Al} \end{aligned}\right\} \qquad 0.020 \lesssim |t| \lesssim 0.035\ \{GeV^2\}$$

Acknowledgements

We wish to thank Prof. W. Jentschke and Prof. P. Stähelin for their continued interest and encouragement in this experiment. We are very much indebted to the DESY Rechenzentrum, the Hallendienst and the synchrotron staff for their excellent cooperation and support. We thank Dr. A. Kanaris and Mr. T. Wynroe for their help during the experiment, we also thank Dr. A. Ladage for the calibration measurement of the beam, Dr. G. Schultze and Mr. F. Selonke for the construction and the test of the Čerenkov counter and Miss H. Freier, Mr. J. Palm, Mr. R. Globisch and our scanning girls for their continuous help.

Literature

(1) This principle was earlier described by Caldwell et al., Rev. Sc. Instr. 36, 283 (1965).

(2) This detection apparatus was also used in an experiment of pion electroproduction by H. Blechschmidt et al. (described in the same conference).

(3) J.D. Jackson, Nuov. Cim. 34, 1644 (1964).

(4) U. Brall et al., Nuov. Cim. 41, 270 (1966).

(5) CEA Bubble Chamber, Phys. Rev. 146, 994 (1966).

(6) L.J. Lanzerotti et al., Phys. Rev. Lett. 15, 210 (1965).

(7) H. Blechschmidt et al., Proc. Int. Symp. on Electron and Photon Interactions, p. 173, Hamburg 1965).

(8) J.G. Asbury et al., Internal DESY-Preprint (July 1967), to be published.

(9) M. Ross and L. Stodolsky, Phys. Rev. 149, 1172 (1966).

(10) S.D. Drell and J.S. Trefil, Phys. Rev. Lett. 16, 552 (1966).

(11) S.M. Berman and S.D. Drell, Phys. Rev. 133, B 791 (1964).

Figure Captions

Fig. 1 Experimental setup.

Fig. 2 Distribution of the difference Δk between measured photon energy and photon energy calculated under the assumption that the reaction $\gamma + A \rightarrow A + \pi^+ + \pi^-$ has occurred.

Fig. 3 $(\pi^+\pi^-)$ mass spectrum for H_2, C and Al target.

Fig. 4 Differential cross section $\frac{d\sigma}{dt}$ as a function of the four momentum transfer square t for H_2, C and Al target.

Fig. 5 Distribution of the ρ^o meson production angles in the center of mass system.

Fig. 6 Angular distribution of the decay pions of the ρ^o meson in the ρ^o rest system:

a) θ_N^* is the angle between the positive pion and the outgoing target nucleus.

b) θ_γ^* is the angle between the positive pion and the incoming photon.

Fig. 7 Mass distribution for events which originate between target and first spark chamber with recoil masses > 1.1 GeV.

Fig. 8 Mass distribution of recoil masses for events with K^{o} meson production.

Fig. 9 $(K^{+}K^{-})$ mass spectrum for all targets.

Fig.10 Distribution of the difference between measured photon energy and the photon energy calculated from the momenta of the K meson pair.

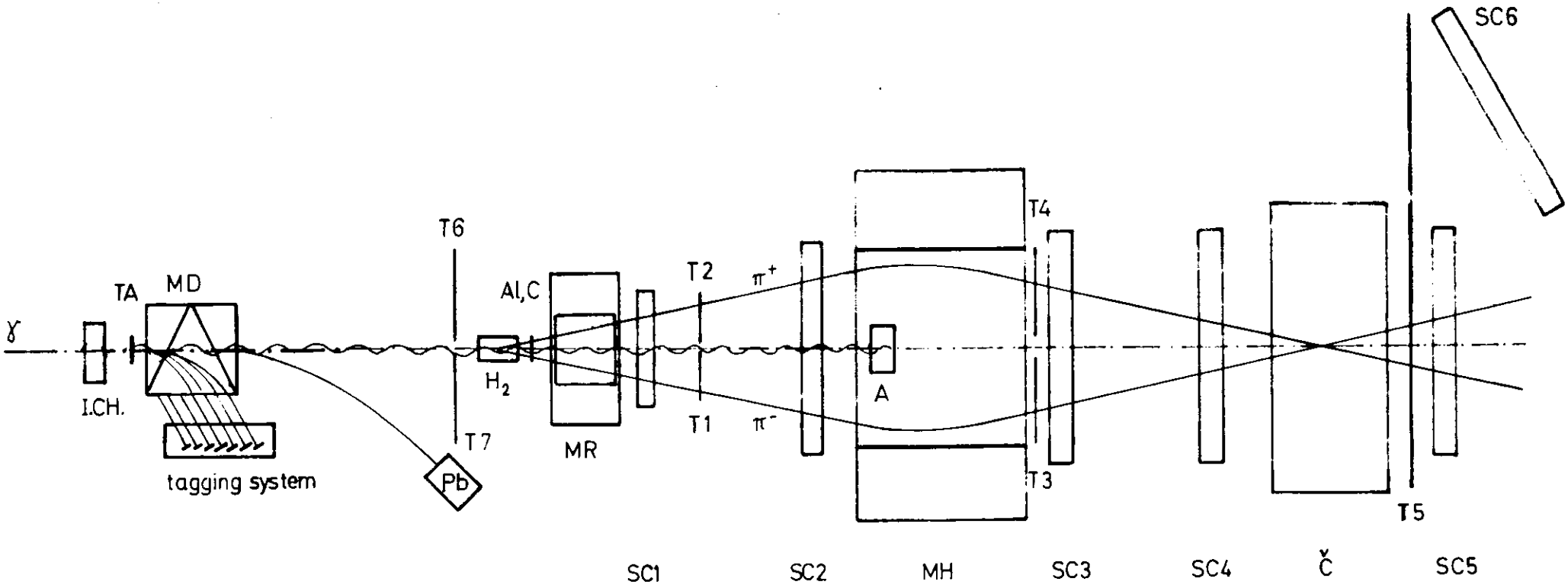
γ
I.CH.
TA
MD
tagging system
T6
T7
Pb
Al,C
H_2
MR
T2
T1
π^+
π^-
T4
T3
A
T5
SC6
SC1
SC2
MH
SC3
SC4
Č
SC5

Fig.1

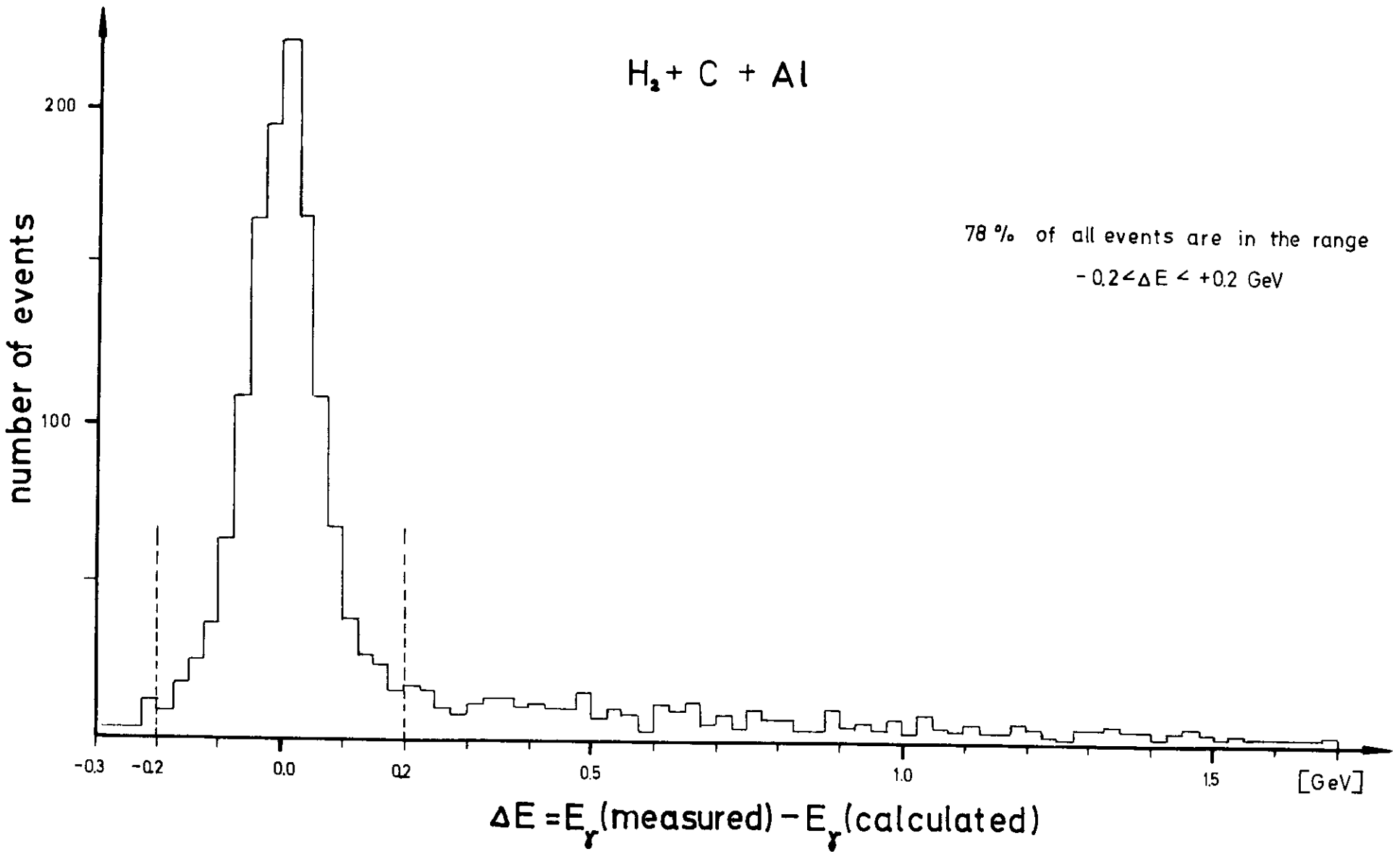
H_2 + C + Al
78 % of all events are in the range
$-0.2 < \Delta E < +0.2$ GeV
number of events
200
100
-0.3
-0.2
0.0
0.2
0.5
1.0
1.5
[GeV]
$\Delta E = E_\gamma$(measured) $- E_\gamma$(calculated)

Fig.2

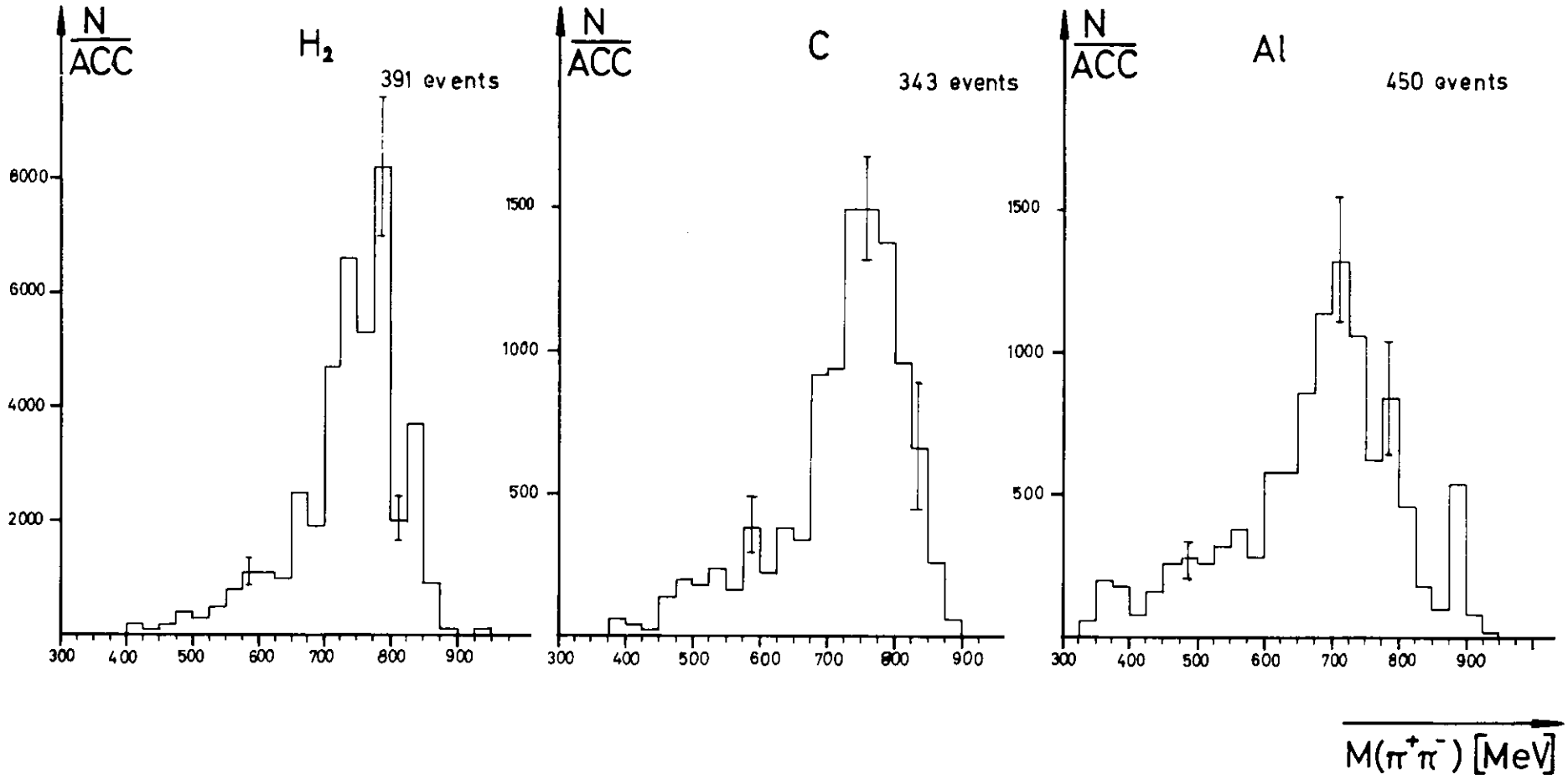
N/ACC
H₂
391 events
8000
6000
4000
2000
300
400
500
600
700
800
900
N/ACC
C
343 events
1500
1000
500
300
400
500
600
700
800
900
N/ACC
Al
450 events
1500
1000
500
300
400
500
600
700
800
900
M(π⁺π⁻) [MeV]

Fig. 3

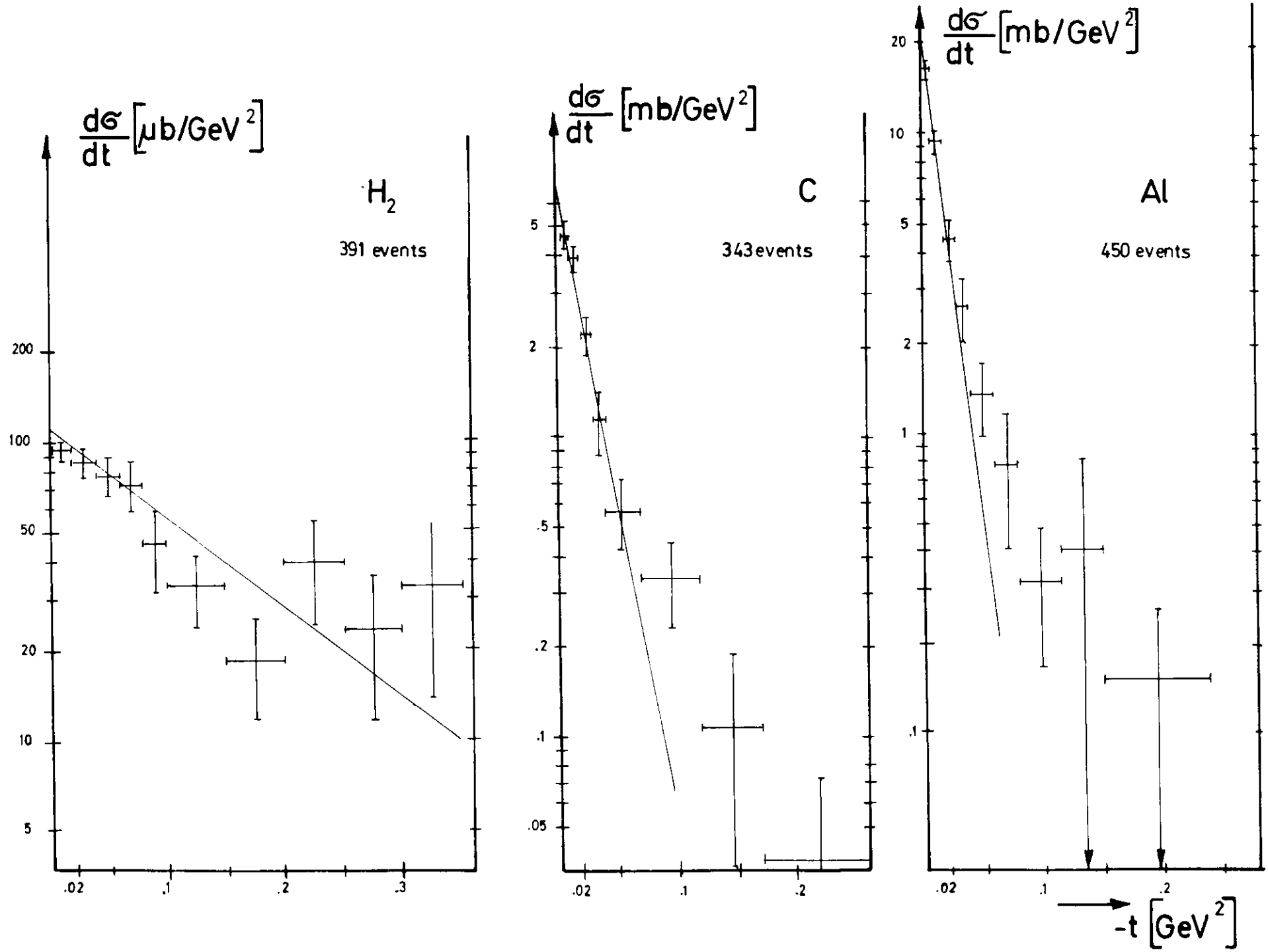
dσ/dt [μb/GeV²]
H₂
391 events
200
100
50
20
10
5
.02
.1
.2
.3
dσ/dt [mb/GeV²]
C
343 events
5
2
.5
.2
.1
.05
.02
.1
.2
dσ/dt [mb/GeV²]
Al
450 events
20
10
5
2
1
.1
.02
.1
.2
-t [GeV²]

Fig.4

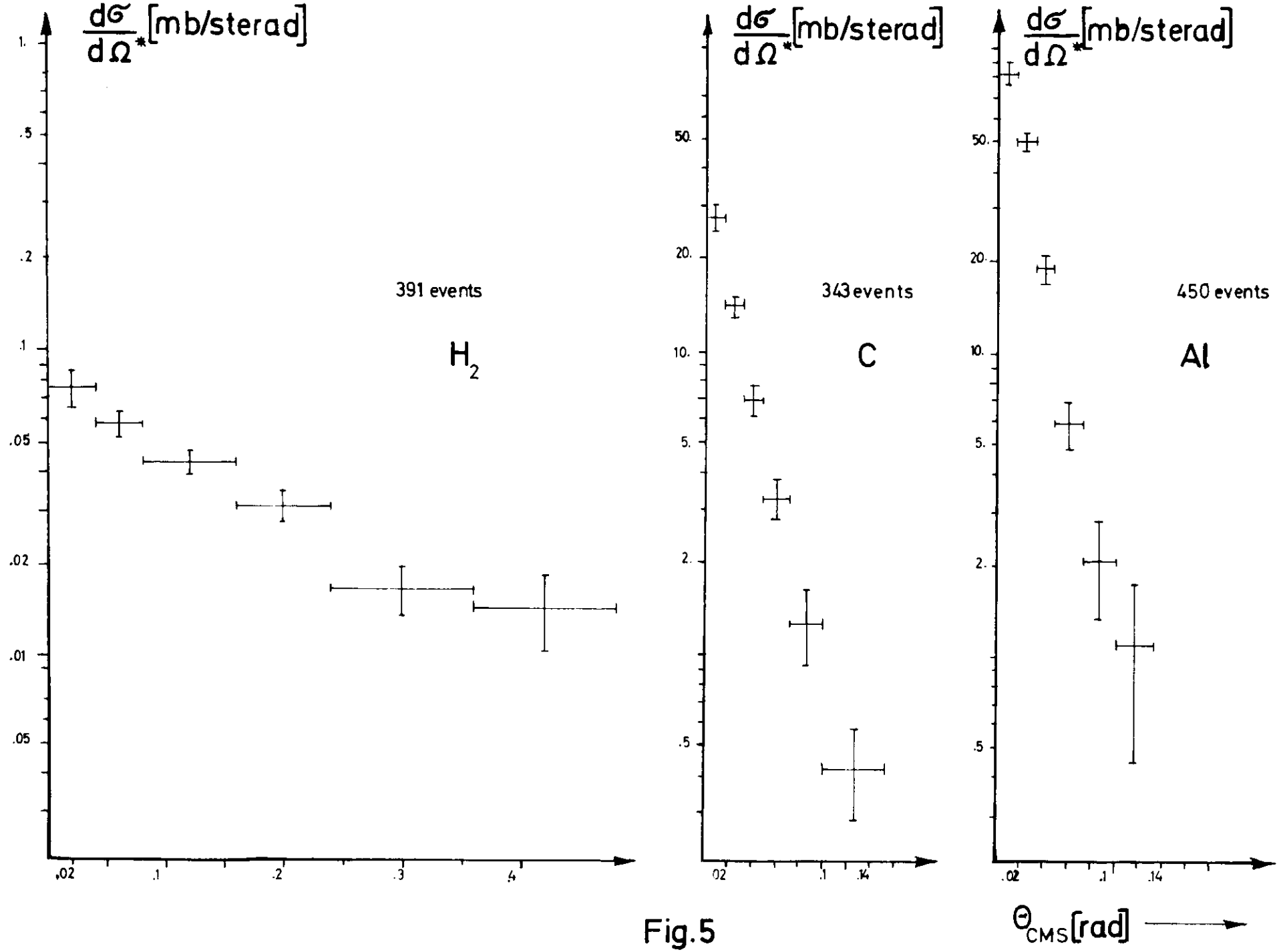
dσ/dΩ* [mb/sterad]
391 events
H2
343 events
C
450 events
Al
Θ CMS [rad]

Fig.5

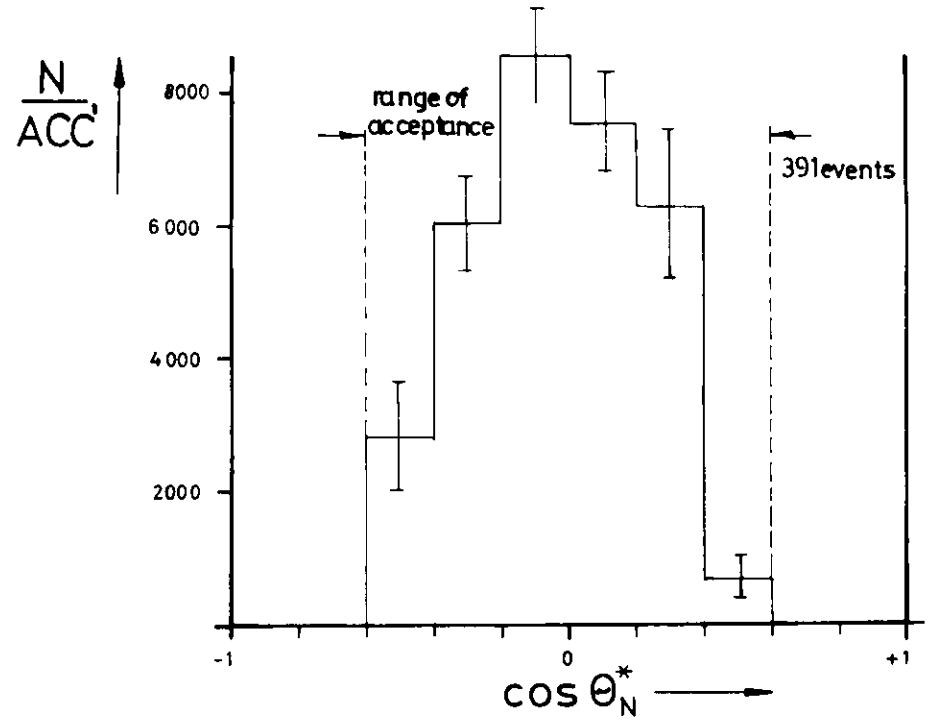
N/ACC
8000
6 000
4 000
2000
range of acceptance
391events
-1
0
+1
cos Θ*N

H_2

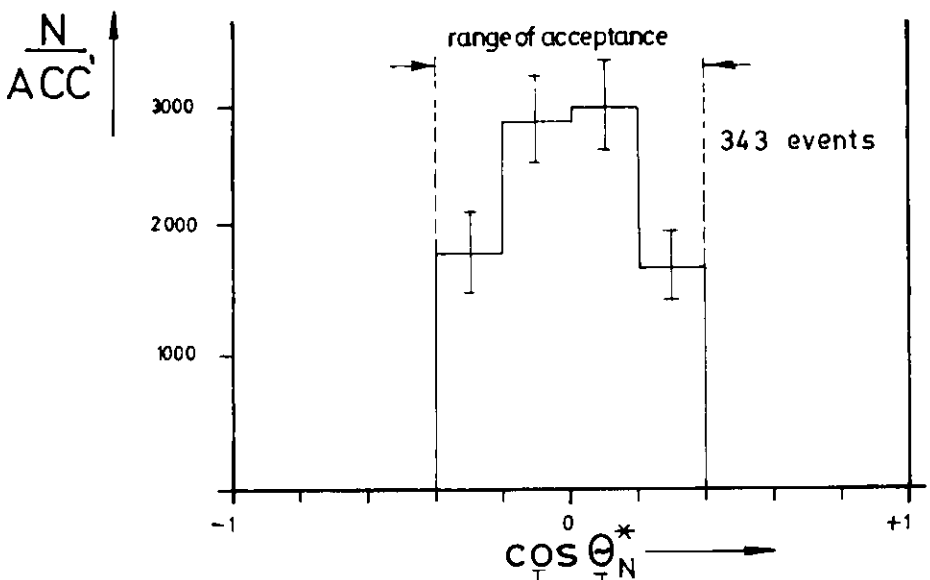
N/ACC
3000
2000
1000
range of acceptance
343 events
-1
0
+1
cos Θ*N

C

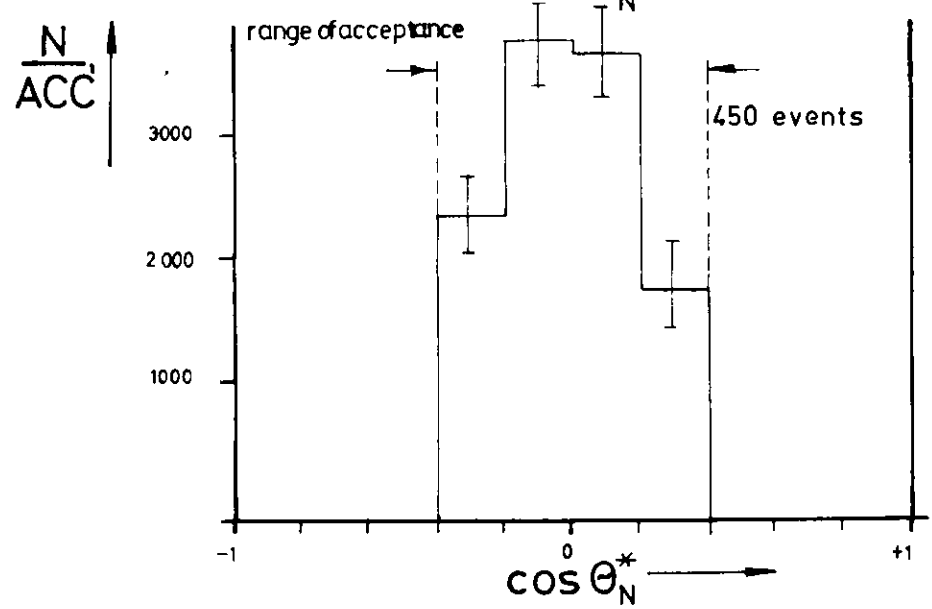
N/ACC
3000
2 000
1000
range of acceptance
450 events
-1
0
+1
cos Θ*N

Al

Fig. 6a

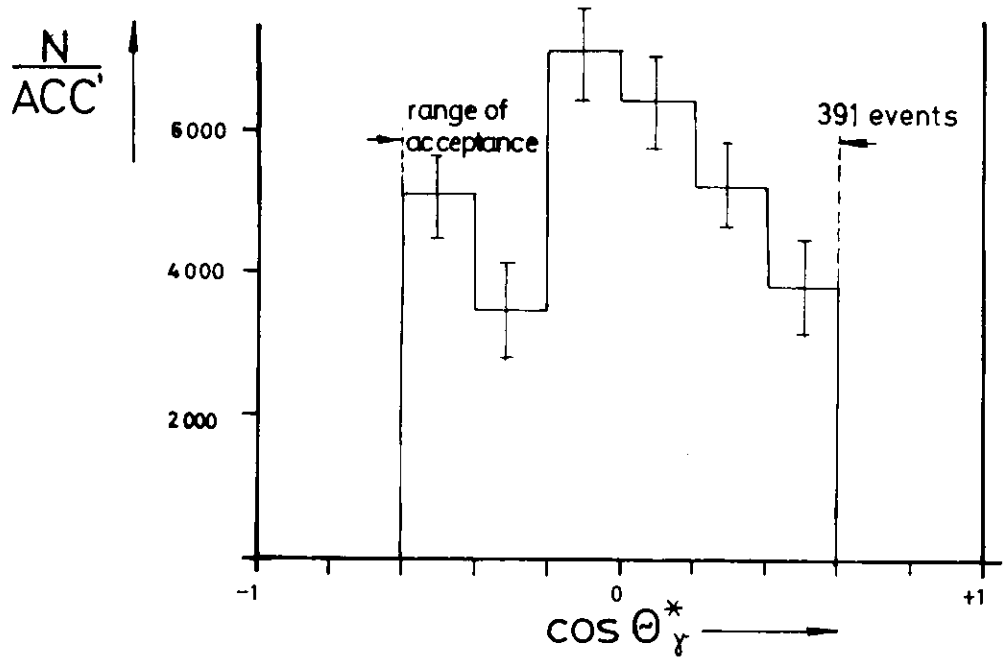
N/ACC'
6000
4000
2000
range of acceptance
391 events
-1
0
+1
cos Θ*γ

H_2

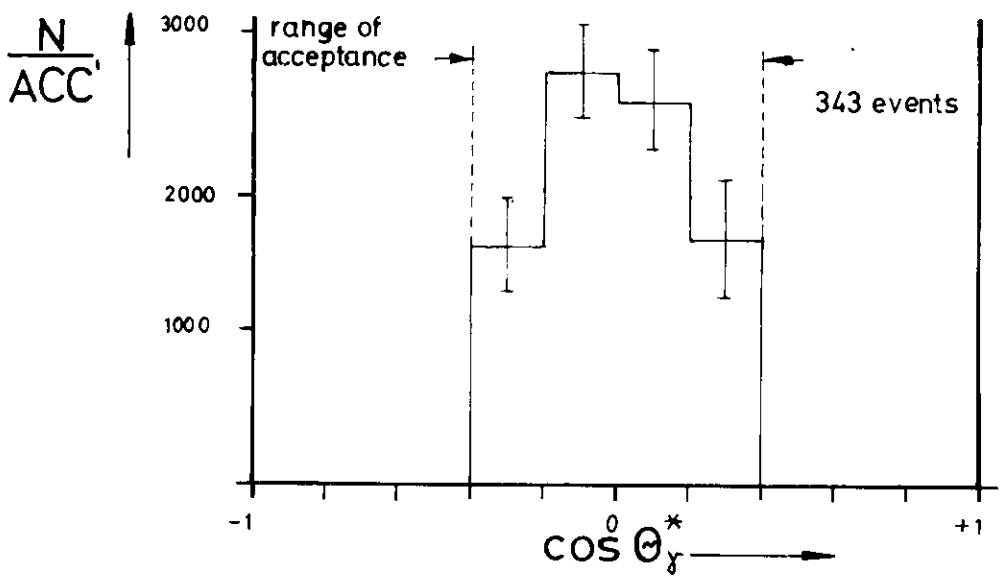
N/ACC'
3000
2000
1000
range of acceptance
343 events
-1
0
+1
cos Θ*γ

C

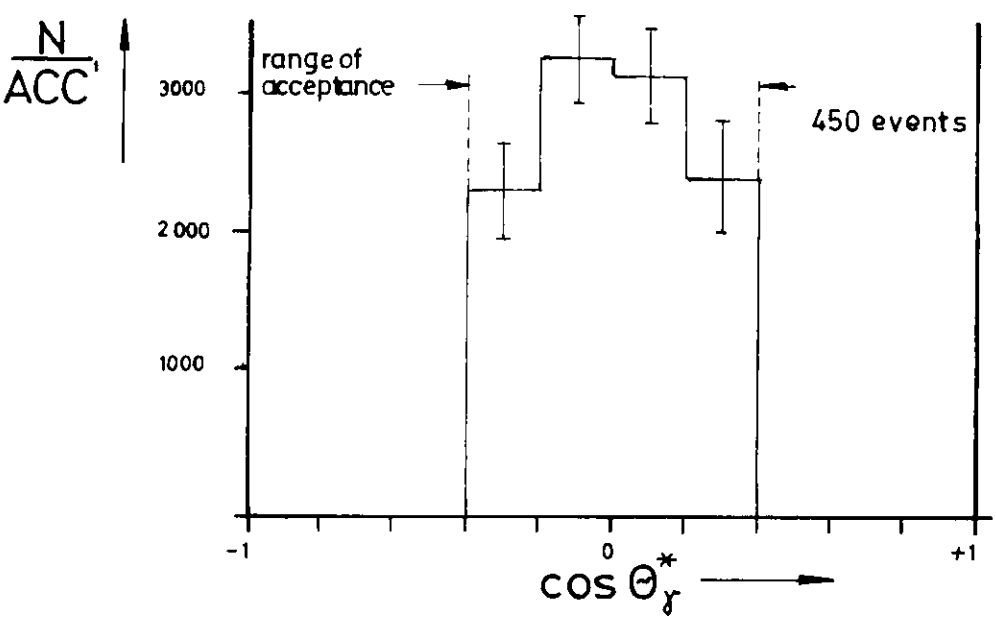
N/ACC'
3000
2000
1000
range of acceptance
450 events
-1
0
+1
cos Θ*γ

Al

Fig. 6b

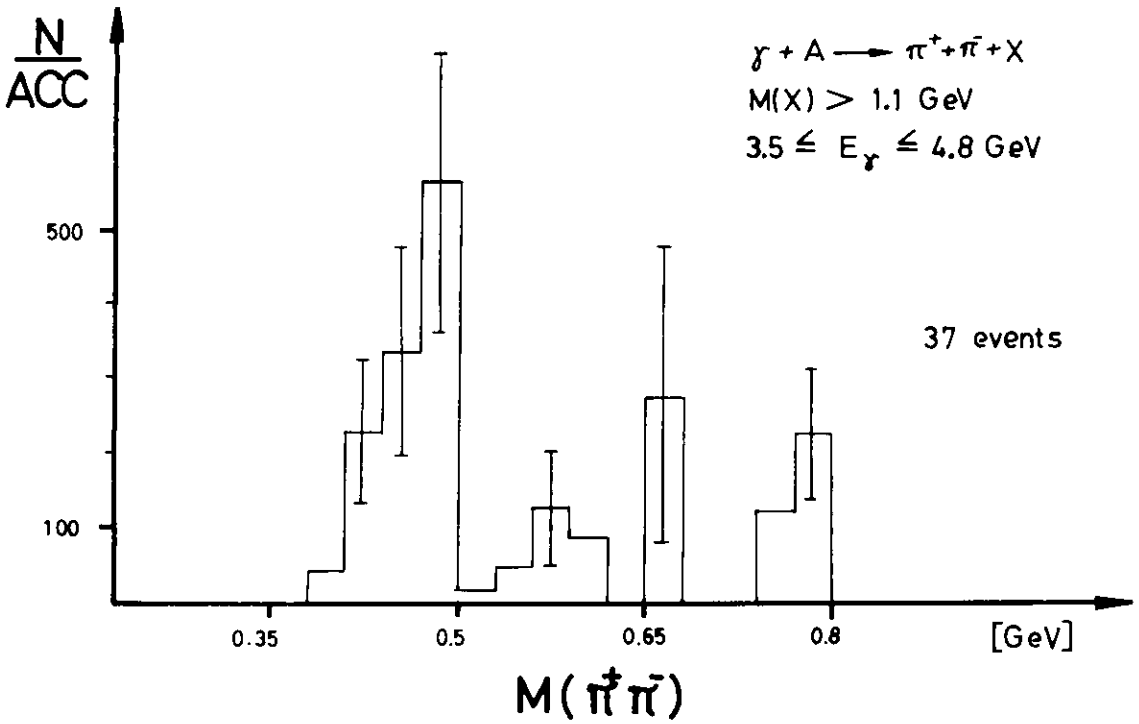
N/ACC
500
100
$\gamma + A \longrightarrow \pi^+ + \pi^- + X$
M(X) > 1.1 GeV
$3.5 \leq E_\gamma \leq 4.8$ GeV
37 events
0.35
0.5
0.65
0.8
[GeV]
$M(\pi^+\pi^-)$

Fig.7

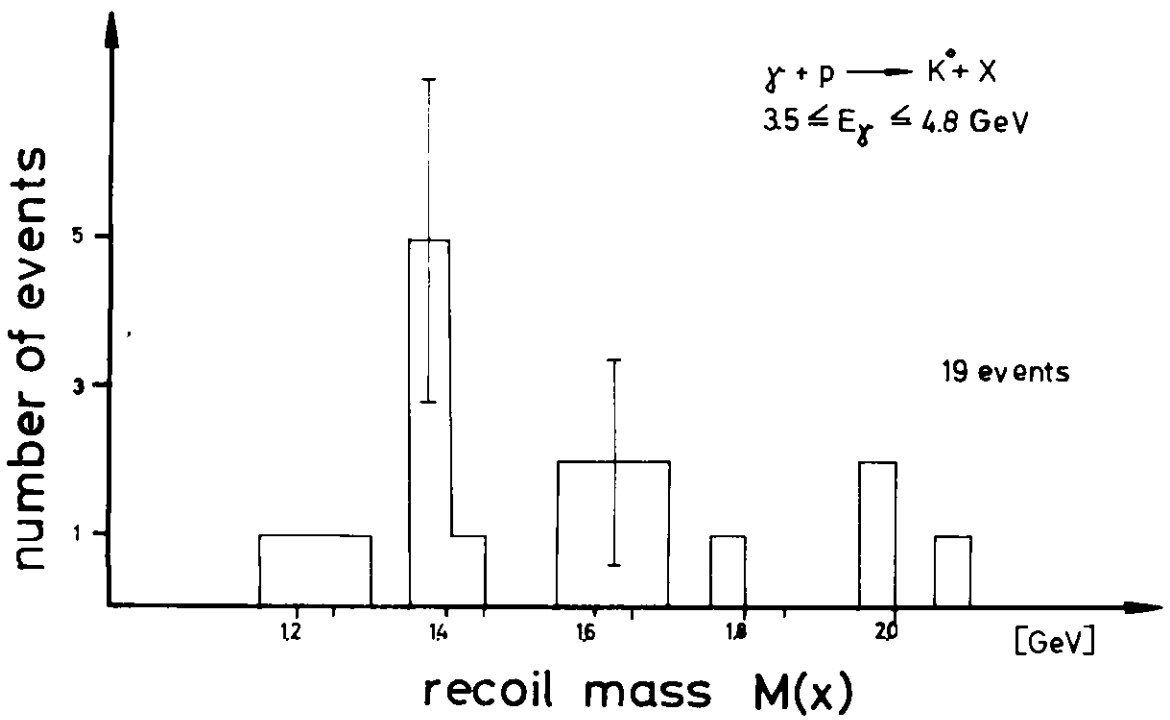
number of events
5
3
1
$\gamma + p \longrightarrow K^\circ + X$
$3.5 \leq E_\gamma \leq 4.8$ GeV
19 events
1.2
1.4
1.6
1.8
2.0
[GeV]
recoil mass M(x)

Fig.8

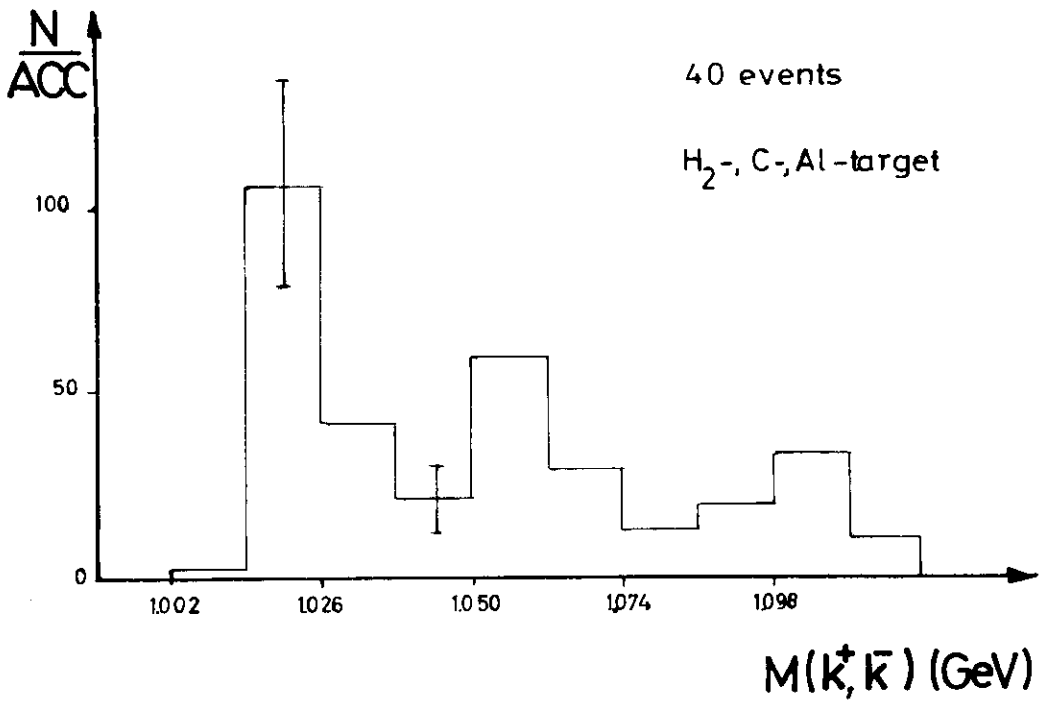
N/ACC
40 events
H_2-, C-, Al-target
100
50
0
1.002
1.026
1.050
1.074
1.098
$M(k^+, k^-)$ (GeV)

Fig.9

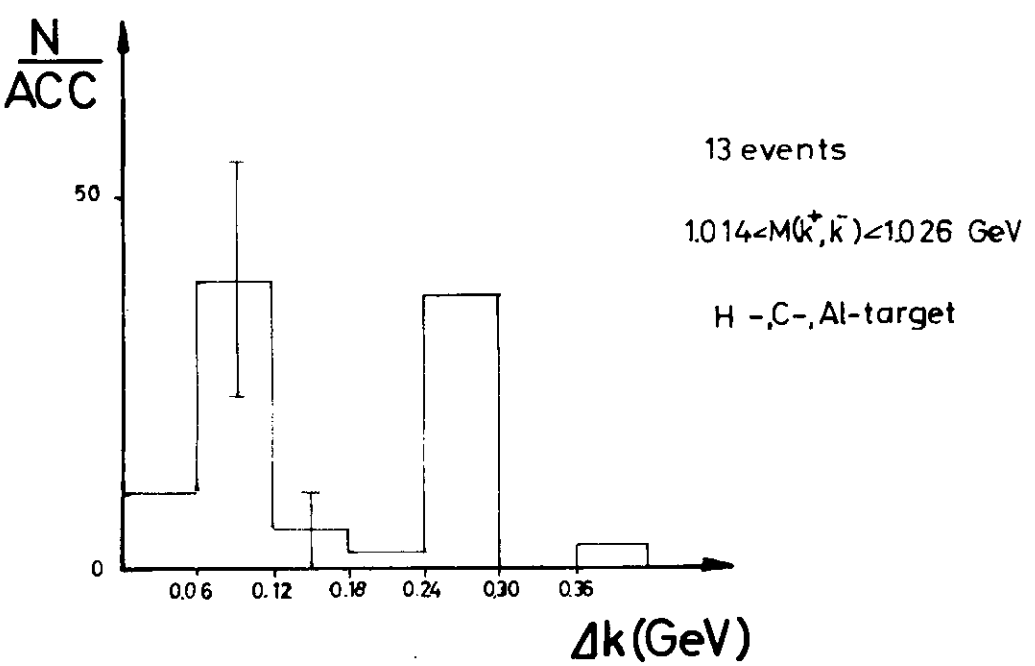
N/ACC
13 events
$1.014 < M(k^+, k^-) < 1.026$ GeV
H -, C-, Al-target
50
0
0.06
0.12
0.18
0.24
0.30
0.36
Δk (GeV)

Fig. 10